ISSN 1067-8212, Russian Journal of Non-Ferrous Metals, 2020, Vol. 61, No. 5, pp. 571–582. © Allerton Press, Inc., 2020.

REFRACTORY, CERAMIC, AND COMPOSITE MATERIALS

Microstructure and Wear Properties of Hot-Pressed NiCrBSi/TiC Composite Materials

S. Islak[a], *, M. Ulutan[b], **, and S. Buytoz[c], ***

[a] *Kastamonu University, Faculty of Engineering and Architecture, Department of Mechanical Engineering, Kastamonu, TR-37150 Turkey*

[b] *Eskişehir Osmangazi University, Faculty of Engineering-Architecture, Department of Mechanical Engineering, Eskişehir, TR-26480 Turkey*

[c] *Fırat University, Faculty of Technology, Department of Metallurgy and Materials Engineering, Elazığ, TR-23100 Turkey*

**e-mail: serkan@kastamonu.edu.tr*

***e-mail: mulutan@ogu.edu.tr*

****e-mail: sbuytoz@gmail.com*

Received March 18, 2020; revised June 29, 2020; accepted July 2, 2020

Abstract—In this study, TiC-reinforced NiCrBSi matrix composite materials were produced using the hot pressing powder metallurgy (PM) technique. The effect of the addition of titanium carbide to NiCrBSi powder in different proportions (5, 10, and 20 wt %) on the microstructure, hardness, relative density, and wear properties of composites was investigated experimentally. NiCrBSi–TiC composites were produced for 10 min at 1000°C with an applied pressure of 45 MPa using a vacuum-assisted automatic hot-pressing machine. The wear behaviors of the composites were compared through dry sliding wear tests. Wear rates and coefficient of friction (COF) values were observed of composites. In addition, the main wear mechanisms are investigated by using SEM and EDS analyses of the worn surfaces. The wear rates of the composites were decreased by increasing the TiC content.

Keywords: NiCrBSi, titanium carbide, friction, metal-matrix composites (MMCs), wear

DOI: 10.3103/S1067821220050053

1. INTRODUCTION

Metal matrix composites (MMCs), which have good wear resistance, hardness, and corrosion resistance are preferred in industry in comparison to non-reinforced alloys [1–3]. Nickel-based alloys are popular as matrix materials because they are resistant to high-temperature conditions. These alloys are particularly used in forming composite layers or coatings on the surfaces of materials. For example, Serres et al. [4] produced NiCrBSi–WC composite coatings by a hybrid plasma/laser process. They found that the process can be applied to simultaneously melt composite materials with high melting temperature and high hardness without the propagation of cracks. Cai et al. [5] formed Ni/TiC composite coatings on AISI 1045 carbon steel substrates by spray plasma spray technology. These composite coatings were mainly composed of TiC, γ-Ni, Cr_7C_3 and CrB and exhibited excellent tribological properties under different loads. Buytoz et al. [6] used NiCrBSi and different proportions of SiC powders to produce the composite coatings on SAE 1030 steel. They observed that the coefficients of friction (COFs) and wear rate of all samples with HVOF coatings were lower than those of the SAE 1030 steel. The increase in the amount of SiC powder had a beneficial influence on the COF and the wear rate of composite layers. Zikin et al. [7] investigated the erosive and impact/abrasive wear behaviour of TiC–NiMo and Cr_3C_2–Ni reinforced NiCrBSi composite hardfacings produced by the plasma transferred arc process. They found a high wear resistance at all test temperatures under both impact/abrasion and erosion conditions. Zhang et al. [8] produced Fe–28Al–5Cr/TiC composites by a hot-pressing process and investigated the dry-sliding tribological performance of these composites in an ambient environment at varying applied loads and sliding speeds. They found that the COF was independent of the TiC amount and applied load but increased from 0.46 to 0.60 with increasing sliding speed under the given testing conditions. The wear resistance increased with increasing TiC content. The enhanced wear resistance is attributed to the high hardness of the composites and the hard TiC phase also plays the role of carrying the load. Zhang et al. [9] also investigated the high-temperature tribological behaviour of Fe–28Al–5Cr alloy

Table 1. Production parameters and composition of composite materials

Sample	Composition, wt %		Production parameters		
	NiCrBSi	TiC	temperature, °C	duration, min	pressure, MPa
S0	100	–	1000	10	45
S5	95	5			
S10	90	10			
S20	80	20			

and its composites containing TiC at different temperatures. They reported that their wear and friction properties improved.

B in the chemical composition of NiBSi- and NiCrBSi-based alloy powders reduces the melting point of the alloy and contributes to the formation of hard phases [10, 11]. Si is added for the purpose of improving nickel mobility. It is reported that Si addition reduces the liquidus temperature of Ni alloy with constant B content [12, 13]. Cr, on the other hand, provides high resistance against oxidation and high-temperature corrosion. In Ni-based alloys, Cr combines with other elements and increases the wear resistance and hardness of the alloy [14]. This renders the powder composition of NiCrBSi a good candidate for a composite matrix material.

Ni alloys are extremely important materials for high temperature applications [15]. Nickel alloys are used in machine parts that are subject to wear and high-temperature corrosion in, for example, the chemical, oil, and glass mould industries, hot work punches, fan blades, sludge disposal members in cement plants, coal boilers, heat exchangers, turbines, pistons, agricultural machinery, medical applications, space craft, nuclear power systems, and thermal processing equipment [16].

TiC is considered to be a strong candidate for the development of cermets due to its high hardness, melting point, chemical and thermal stability, and wear resistance. TiC also exhibits good melt wettability by many metallic binders such as Ni, Co, Al, Cu, Fe [17], and steel matrix [18]. Its beneficial contribution is most likely associated with the enhancement of the mechanical properties and wear resistance at high temperatures [19]. TiC–Ni based cermets were considered as alternatives to WC-based hard metals as cutting set materials. The first TiC–Ni materials were actually formed of Ni, Mo, and TiC, yet they were quite brittle. Hardness increases in line with the amount of TiC, while Mo is usually added as Mo_2C in order to obtain a good level of wettability with the ceramic phase. Ni, on the other hand, is used to obtain better toughness [20].

MMCs can be produced by methods such as casting technologies, powder metallurgy and coating technologies. The properties of composites produced after these methods are different. In particular, the powder metallurgy method is used extensively in the production of MMCs due to the advantages such as providing homogeneous distribution of reinforcing elements in the matrix, obtaining a smoother surface and no unwanted phases in the matrix-reinforcing interface [21–23].

The purpose of the present study is to evaluate the microstructure and wear properties of NiCrBSi–TiC composite material produced through the hot-pressing PM technique. For this purpose, the microstructure, phase compositions, and worn surfaces of NiCrBSi–TiC composite materials were examined through optical microscopy, scanning electron microscopy, X-ray diffraction (XRD).

2. MATERIALS AND METHODS

NiCrBSi-based TiC-reinforced MMCs were produced through hot pressing (HP) method. Having a grain size of -53 ± 20 μm, the chemical composition of NiCrBSi powder (in terms of weight percentage) is 4.5% Si, 4.5% Fe, 3.3% B, 14% Cr, and 0.75% C, with Ni making up the remainder, while the chemical composition of TiC with a grain size of 10 μm is 19.28% C and 80.72% Ti. Varying contents (weight percentages) of TiC grains were added to the NiCrBSi matrix composites at the parameter values shown in Table 1. Figure 1 shows the SEM photography of the NiCrBSi and TiC powders used in the production of the composites. As can be seen from the pictures, NiCrBSi powders are partially spherical, while TiC grains have a sharp-edged appearance.

Powders were mixed at a speed of 20 rpm, for 45 min in a Turbula mixer (Celmak Group 7T, Turkey). Powders mixed at varying rates were pressed and

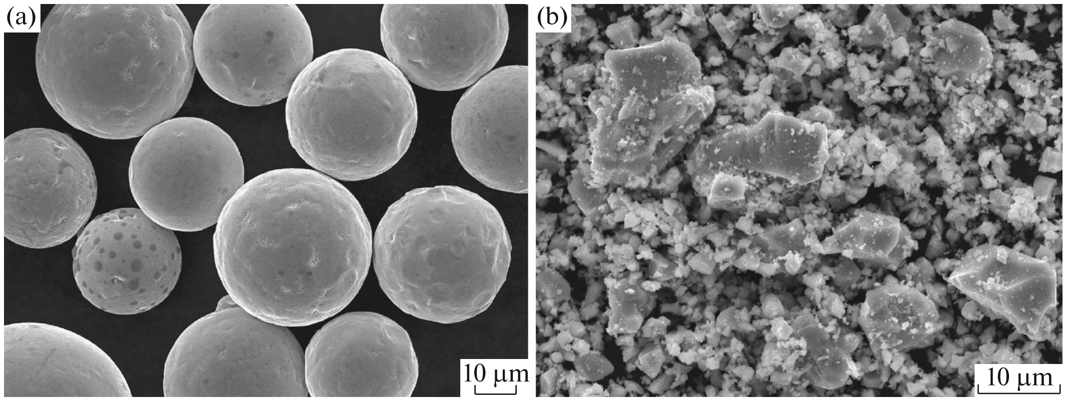

Fig. 1. (a) SEM micrographs of NiCrBSi powder and (b) TiC powder.

sintered with a Diex brand vacuum-supported hot press. The powders inserted between graphite moulds were condensed at a temperature of 1000°C and a pressure of 45 MPa for 10 min. After hot pressing, the final dimensions of the samples are designed as 10 × 10 × 20 mm.

Relative density measurements of the samples were carried out in line with Archimedes' principle. The microhardness of NiCrBSi–TiC composites was measured by using a Vickers hardness device under a load of 100 gf. OM and SEM were used for the microstructural examinations of the composite materials, and phase analyses were carried out by XRD and EDS. XRD analyses were carried out using Bruker AXS D8 advance equipment at 30 kV with 15 mA of Cu $K\alpha$ radiation and a Rigaku Geigerflex X-ray diffractometer. Wear tests of NiCrBSi–TiC composites were carried out using a CSM tribometer device (ASTM G133 standard). Wear test conditions are given in Table 2. ∅3 mm 94% WC + 6% Co Certified spherity ball (Redhill Precision Specialty Balls Company) was used. The hardness and modulus of elasticity are 1800 HV and 640 GPa respectively. Worn surfaces of samples were examined by SEM- EDS analyses.

3. RESULTS AND DISCUSSION

3.1. Microstructure

SEM photographs of the NiCrBSi matrix TiC-reinforced composite materials produced by means of powder metallurgy are presented in Fig. 2. In the microstructure of the NiCrBSi that was not reinforced with TiC, it can be observed that NiCrBSi grains completely merge with each other and therefore a high rate of neck formation occurs between the grains. Within the light coloured matrix, the rods form spherical and quadrangular structures. Figures 2b–2d show the microstructure of composite materials reinforced with 5, 10, and 20% TiC, respectively. As TiC is added to the NiCrBSi matrix, the presence of TiC phases also becomes apparent in the microstructure. Differences in the distribution within the microstructure were observed with the addition of TiC. TiC particles were formed on the boundaries of NiCrBSi particles and as the amount of added TiC increased, they surrounded the matrix in the form of a net.

In composite materials, homogeneous or heterogeneous distribution of reinforcing elements in the matrix has an extremely important effect in terms of physical and mechanical properties of composite materials [24, 25] Figure 3 shows images of the SEM-MAP analysis of sintered NiCrBSi–10 wt % TiC composite. The SEM image illustrates a fairly homogeneous distribution of TiC in NiCrBSi. The EDS image shows the main spectra of Ni, Cr, B, Si, and Ti elements at all locations. The level of Ni was considerably higher compared to other elements. The titanium spectrum represented the presence of TiC.

Table 2. Wear test conditions of composite materials

Linear speed, cm/s	5
Normal load, N	3
Sliding distance, m	50
Wear trace, mm	7
Ambient temperature, °C	25
Ambient moisture, %	35
Data collection rate, Hz	10
Counter material	94% WC + 6% Cobalt
Counter material diameter, mm	3

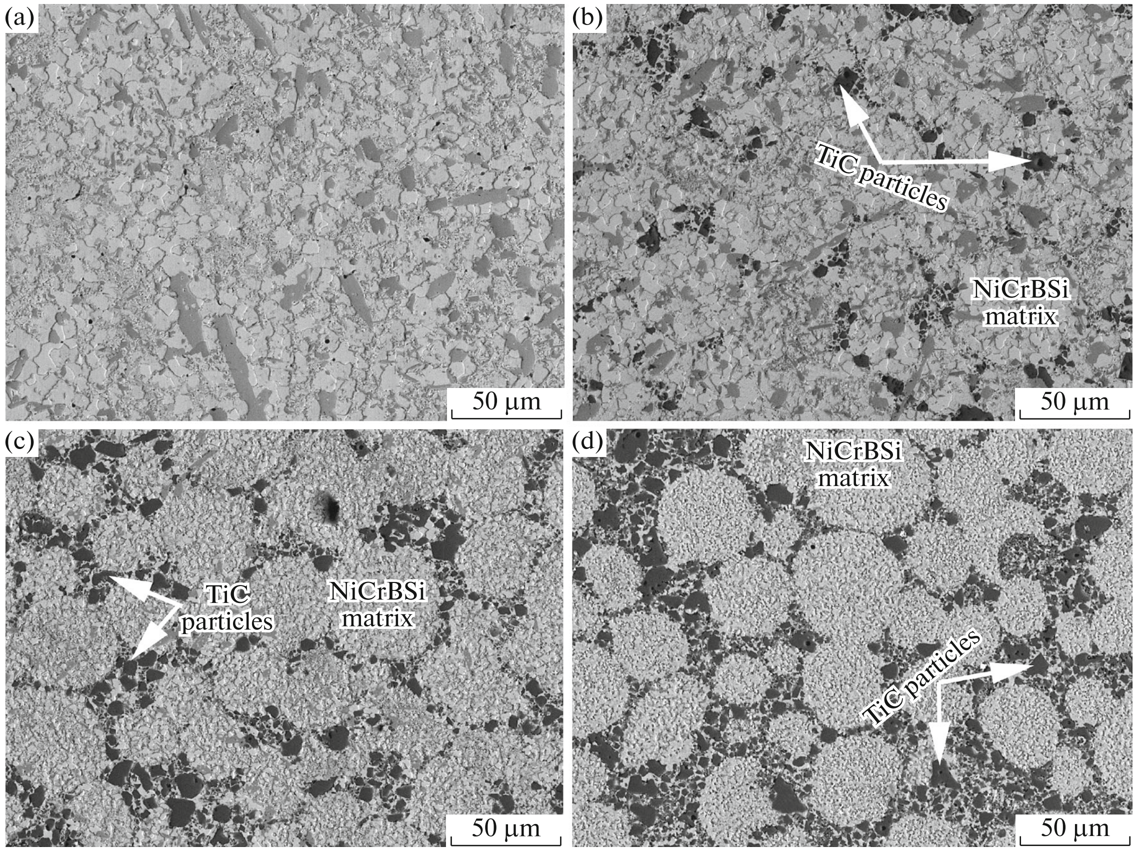

Fig. 2. SEM micrographs of NiCrBSi–TiC composite materials: (a) without TiC addition, (b) 5% TiC, (c) 10% TiC, and (d) 20% TiC.

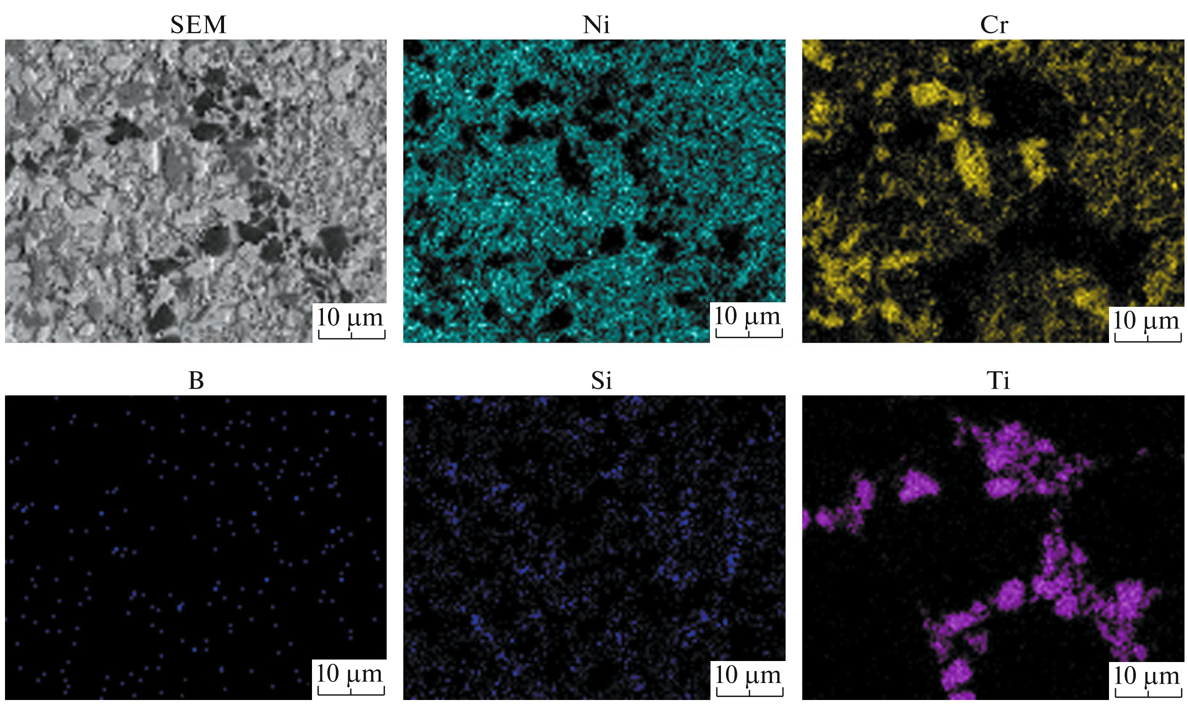

Fig. 3. SEM-MAP analysis showing uniform phase distribution of Ni, Cr, B, Si, and Ti elements for NiCrBSi–10 wt % TiC composite.

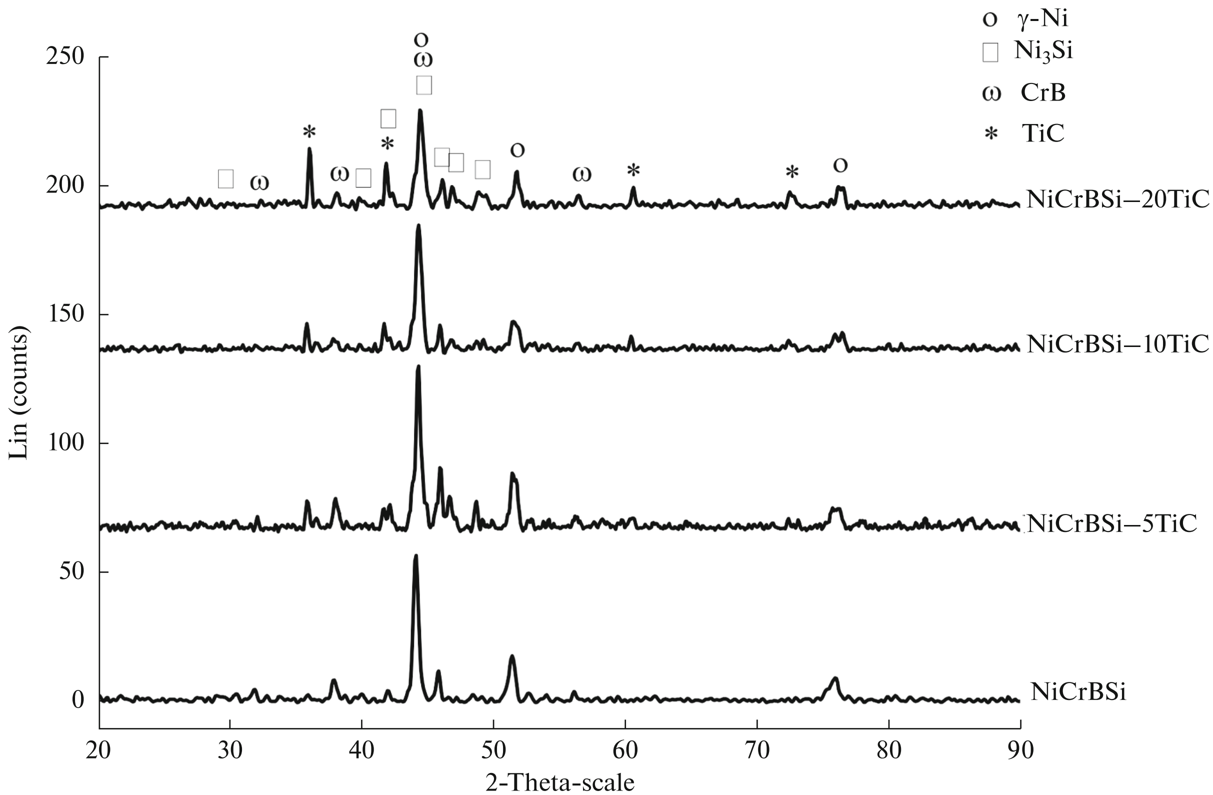

Fig. 4. XRD diffractograms of NiCrBSi–TiC composites.

Figure 4 shows the XRD diffractograms of NiCrBSi and NiCrBSi–TiC materials. According to the analysis results, γ-Ni, Ni_3Si, CrB, and TiC phases were formed in the structure. Silva et al. [26] reported the formation of γ-Ni, Ni_3Si and CrB phases in their study on the wear and microstructure properties of NiCrBSi coatings. Since there is no chemical reaction between the TiC particle and the NiCrBSi particle, no new Ti-containing phase has been formed. This can be explained by the fact that the sintering temperature is insufficient for this chemical reaction. This has also been reported in studies in the literature. Islak et al. [27]. In their study on Cu–TiC composite materials, they found that a phase did not occur due to insufficient sintering temperature between Cu and Ti. The intensity of the TiC peak in the diffractograms increased in line with the increasing TiC amount.

3.2. Density and Hardness

The relative densities of NiCrBSi and NiBSi–TiC composites determined through the use of Archimedes' principle are presented in Fig. 5 according to the amount of TiC added. As the amount of TiC addition increases, the relative densities of the composites exhibited decreases. While the relative density of NiCrBSi was 98.24%, the relative densities of composites obtained with the addition of 5, 10, and 20% TiC were 95.87, 92.56, and 88.34%, respectively. This is due to the fact that reinforcement particles reduce the compactibility of composite powders. Another reason for this is the effect of reinforcement particles that pre-

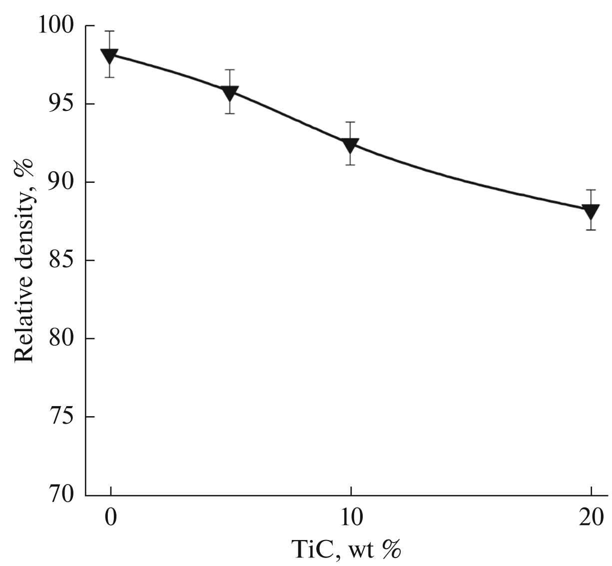

Fig. 5. Relative densities of NiCrBSi–TiC composites depending on TiC addition.

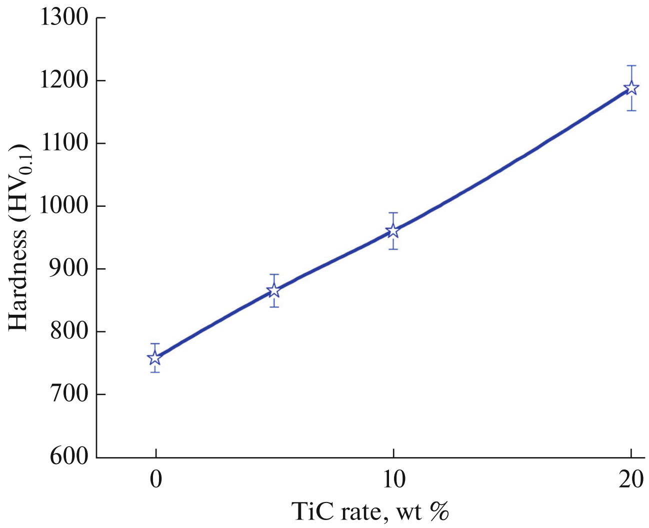

Fig. 6. Hardness of NiCrBSi–TiC composites.

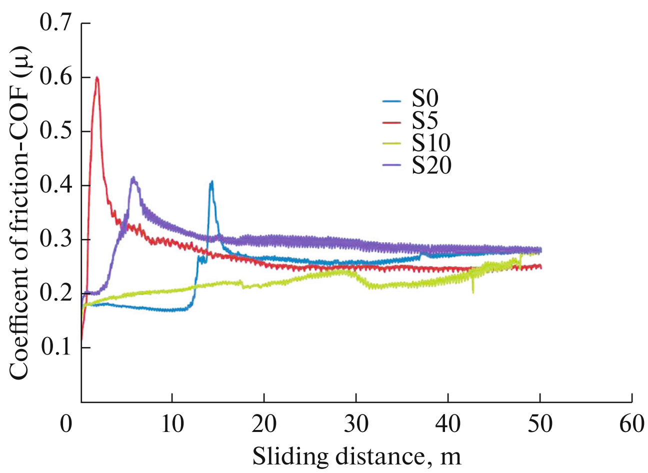

Fig. 7. Diagram of coefficient of friction versus sliding distance of NiCrBSi–TiC composites.

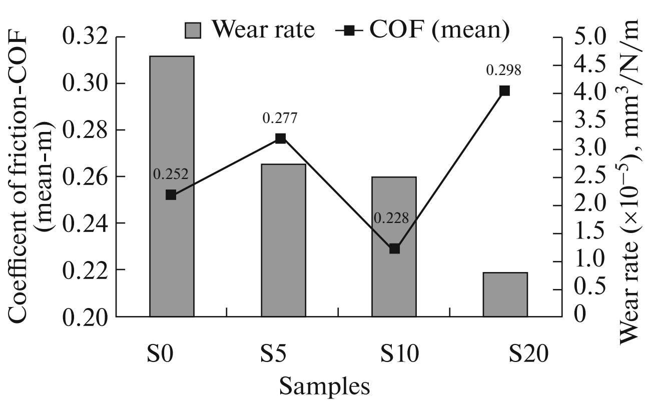

Fig. 8. Graph of average coefficient of friction and wear rates of NiCrBSi–TiC composites.

vent the rearrangement of composite powders during the sintering of the composite due to the considerable difference between the melting points of the reinforcement particles (3160°C) and that of the matrix (~1100°C) [28] because, although the matrix can be diffused more easily between reinforcement particles with the addition of a smaller amount of reinforcement, as the amount of reinforcement increases the reinforcement particles form a barrier that prevents diffusion. This in turn results in decreases in the relative densities of the composites [29, 30].

The hardness values of the obtained NiCrBSi–TiC composites according to the amount of TiC addition are presented in Fig. 6. As the amount of TiC added increases, a significant increase in composite hardness takes place. The hardness values of NiCrBSi-TiC composites vary within the range of 867 to 1188 $HV_{0.1}$. It is possible to assert that this increase of hardness is triggered by the distribution of titanium carbide within the matrix. The hard reinforcement elements in the matrix have an effect preventing dislocation movement. This causes an increase in the hardness of the composite. In addition, the high natural hardness of the elements forming the composite material, especially the reinforcements, causes an increase in the hardness of the composite according to the mixing rule. The increase in the amount of hard reinforcements causes an increase in the hardness of the composite [31].

3.3. Wear and Friction Tests

The COF values obtained as a function of sliding distance for the four samples with varying rates of TiC reinforcement are presented in Fig. 7. As can be seen from this figure, after the distance reaches 15 m, an almost fixed variation of the COF can be observed for all samples. From the start of the tests, rapid increases in the COFs are observed within the first 15 m of sliding distance. These increases take place due to the abrasive effect of the weak oxides, which become crushed on the sample surfaces. In addition, the hard TiC particles separated from the surface of the composite material also create the same effect. The hard composite surfaces and the high load-bearing capacity of the γ-Ni matrix structure seen in all samples reduce the negative effects of these particles on wear. For this reason, the amount of reinforcement used and the matrix become very important in the determination of wear characteristics.

In composites, wear rates need to be considered together with the COF. Figure 8 shows both the average COFs and wear rates. Examination of Fig. 8 shows that the COFs obtained for all samples have rather low values such as 0.25 and 0.3 μ. Although the sample S0 (pure NiCrBSi) exhibited a relatively low COF of 0.25 μ, it exhibited the highest wear rate, with a value

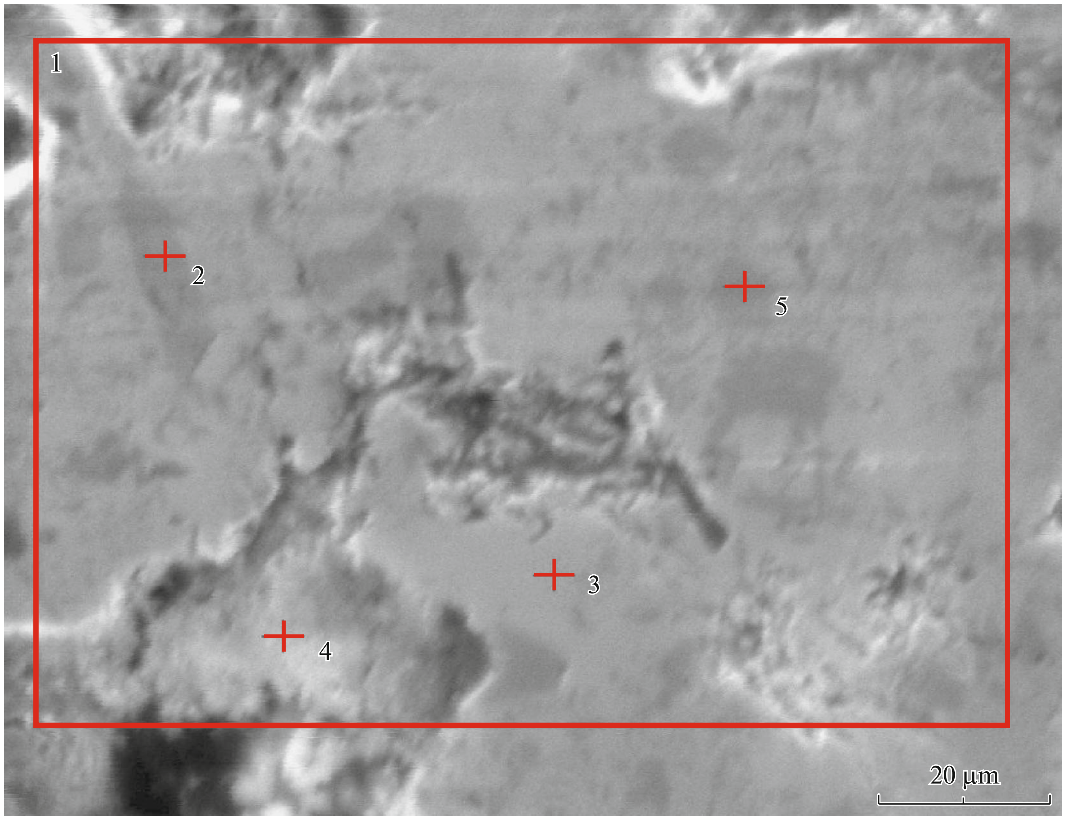

Component	EDS analyses (wt %)				
	Square-1	Point-2	Point-3	Point-4	Point-5
O	3.130	4.496	0.254	24.543	3.319
W	7.722	4.218	7.584	21.188	5.472
C	2.894	2.800	0.000	11.514	0.292
Si	3.900	1.111	0.074	2.294	3.071
Cr	21.310	69.082	8.131	10.889	34.822
Ni	60.902	18.216	83.742	29.399	51.852
B	0.000	0.000	0.000	0.000	0.000
Ti	0.143	0.078	0.215	0.172	0.172
Total	100.000	100.000	100.000	100.000	100.000

Fig. 9. SEM photograph and EDS analysis of the worn surface of S0 composite sample.

of 4.66×10^{-5} mm^3/N m. Although the average COF value in the sample S5 increased to ~0.28 μ, the wear rate decreased to 2.73×10^{-5} mm^3/N m. The sample S10 exhibited the lowest average COF of ~0.23 μ. The wear rate of this sample was determined as 2.50×10^{-5} mm^3/N m; in other words its wear resistance in comparison to the non-reinforced sample approximately doubled. As expected, the sample S20 had the lowest wear rate in all of the samples. This situation was enabled by the adding highest TiC reinforcement ratio. As a matter of fact, the wear rate of this sample decreased to ~0.8×10^{-5} mm^3/N/m which this wear rate was nearly six times lower than non-reinforced sample. However, the average COF for this sample reached the highest value of ~0.3 μ. Examination of the wear distance diagram of this sample (Fig. 7) shows that its friction coefficient, which was 0.2 μ at the early period of the test, increased suddenly and sharply. Due to highest TiC reinforcement ratio, hard TiC particles separated from the surface involved into contact point during the wear test and behave as abrasive third body. This occasion deteriorate the friction behavior of this sample and exhibit highest mean COF values in all samples.

Figures 9–12 show the SEM photographs and EDS analyses of the worn surfaces of composite materials. Examination of the worn surface of the S0 sample (Fig. 9) shows the presence of diverse combinations of microstructures formed through the effect of the NiCrBSi particles. The oxides that formed on the surface are considered to have created an effect that reduces the COF [32, 33]. Also, the W element found in the analyses came from the counter object. This in turn is an indication that the hard structures in the sys-

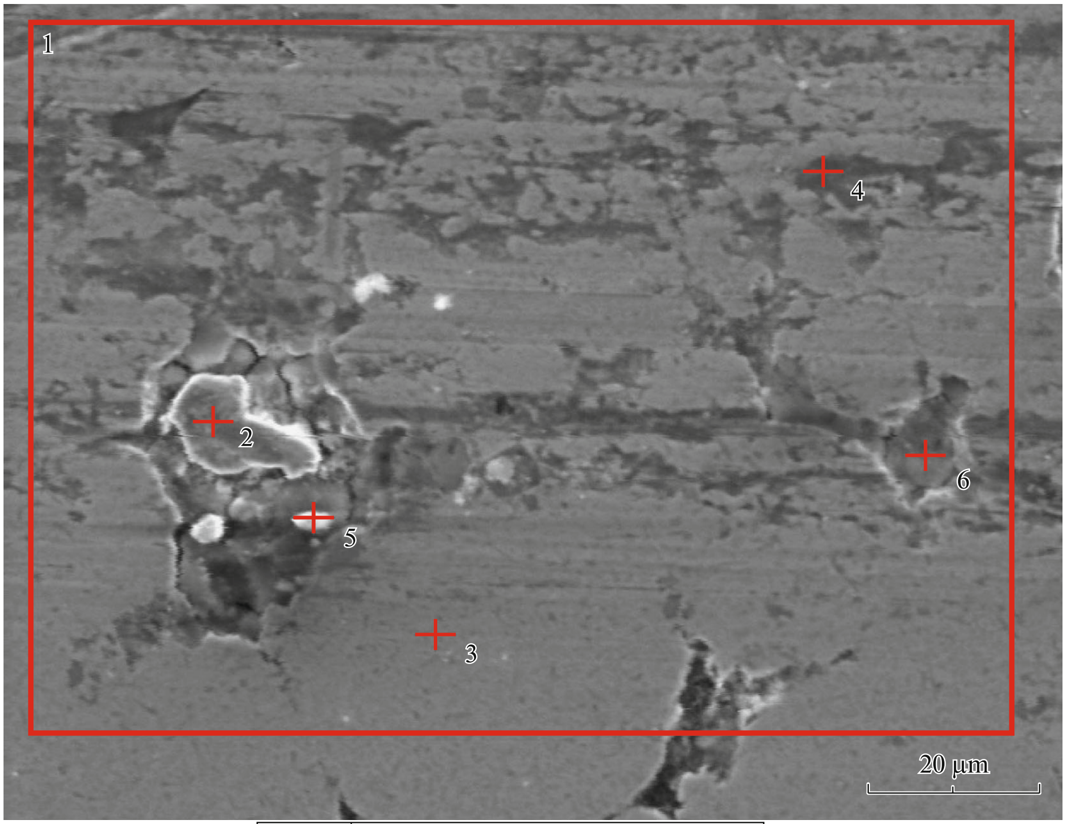

Component	EDS analyses (wt %)					
	Square-1	Point-2	Point-3	Point-4	Point-5	Point-6
O	5.851	4.765	0.777	17.001	10.250	30.304
W	9.396	6.710	9.678	5.901	10.856	4.921
Ti	3.577	0.743	0.133	0.790	4.994	7.628
Cr	13.611	33.040	8.029	10.075	11.902	8.700
B	0.000	0.000	0.000	0.000	0.000	0.000
Si	2.552	1.068	3.738	3.834	1.686	3.527
Ni	62.981	47.493	76.673	60.594	55.728	59.204
C	2.032	6.181	0.972	1.805	4.585	5.717
Total	100.000	100.000	100.000	100.000	100.000	100.000

Fig. 10. SEM photograph and EDS analysis of the worn surface of S5 composite sample.

tem, particularly chromium carbides (point 2) have worn the counter object. At point 4 in Fig. 9, it is seen that the wear debris of the area with high oxide and W content is filled into the hollows of the surface. The deep hollows on the surface confirm the high level of wear loss that took place in this sample. The fact that in this sample there was no reinforcement that would reduce the abrasive effect of the counter object increased the wear loss of the sample. However, the hollows that formed on the surface reduced the contact surface and resulted in a low COF.

Smaller hollows and wear particles are observed on the worn surface of sample S5 (Fig. 10). Also, ploughing effects can be seen which caused by hard particles partially containing Ti–C–O elements. These tribochemical oxides are formed during the tests were observed in surface analyses of the same sample (Fig. 10, point 6). Similar formations can be also seen at points 2 and 5. In spite of this formations, the contact surface area of this sample remained the stable during the wear test and these ruptured oxide formations moves between the contact surfaces freely. This occasions caused to increase the COF.

Figure 11 shows the worn surface of the composite sample S10. The abrasive effects on the surface of this sample, which has the lowest average COF, decreased substantially. Chromium (point 2) and titanium (point 6) carbides are clearly visible on the surface. With the support of these carbides and the lubricant effect of tribo-oxides with titanium content, both the COF and the wear amount decreased. The lubricant effects of titanium oxides are known [34–36].

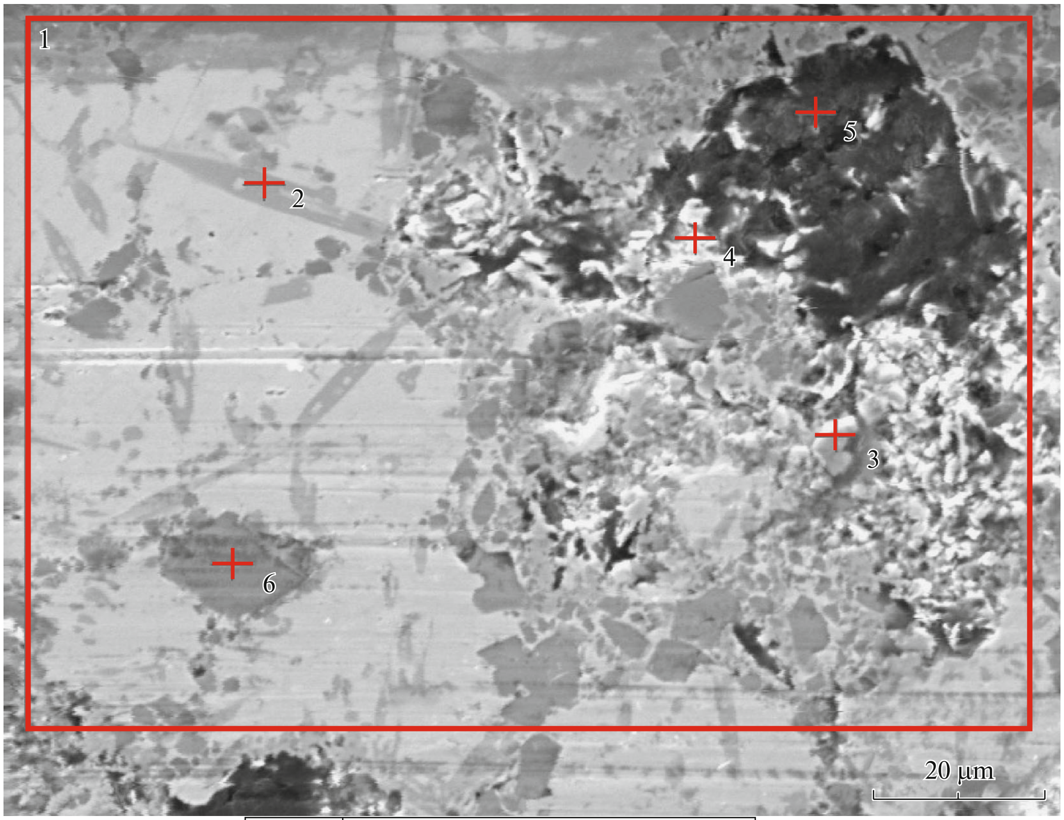

Component	EDS analyses (wt %)					
	Square-1	Point-2	Point-3	Point-4	Point-5	Point-6
O	2.566	4.005	17.453	1.785	5.321	1.398
W	10.813	5.087	15.690	5.327	13.644	4.265
C	16.287	5.137	9.817	26.410	---	6.125
Ti	12.761	0.248	27.347	3.468	4.414	85.473
Cr	14.330	81.182	2.737	32.733	31.453	0.548
B	0.000	0.000	0.000	0.000	0.000	0.000
Si	1.807	0.469	2.182	0.335	4.370	0.342
Ni	41.436	3.862	24.775	29.942	40.798	1.850
Total	100.000	100.000	100.000	100.000	100.000	100.000

Fig. 11. SEM photograph and EDS analysis of the worn surface of S10 composite sample.

Figure 12 shows the SEM photograph and EDS analyses of the worn surface of the S20 sample. It is observed that the abrasive effects and oxides on the sample surface are less visible due to highest TiC ratios as 20%. Due to the high TiC content, the presence of third particles in the intermediate surface increased. Free movements of these particles in the intermediate surface and their contact with the counter body increased the COF. This situation can also be confirmed by the examination of Ti–W contained particles on the surface (Fig. 12, point 3). Despite this situation, the lowest wear rate was observed in this sample due to its high level of bulk hardness which has a highest TiC reinforcement.

4. CONCLUSIONS

In the present study, composite materials were produced by adding TiC reinforcement at four different rates to NiCrBSi. Composites were obtained through hot pressing and sintering under vacuum. It is possible to use these materials in various applications with the obtained values of hardness, wear, and COF.

As a result of the XRD analyses, it was determined that the composites are formed as γ-Ni, Ni_3Si, CrB, and TiC phases. The relative density of the composites is inversely depend on the ratio of the TiC content. On the other hand, hardness values were increased substantially with the increasing TiC rate.

Average COF values of the composites were found to be relatively low nearly as 0.3. Significant decreases in wear rates were observed in TiC reinforced composites samples. Although, the lowest wear rate was observed in the highest TiC reinforced sample, average COF values of the sample measured as highest. This case explained by the fact the TiC particles sepa-

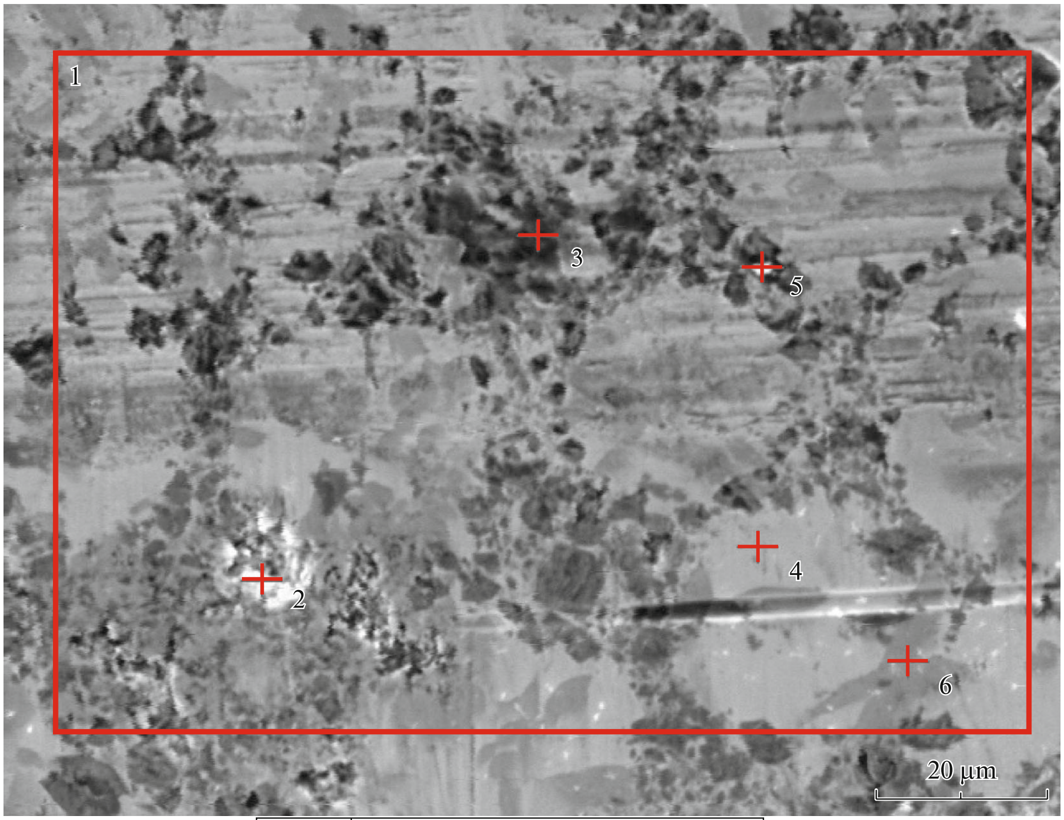

	EDS analyses (wt %)					
Component	Square-1	Point-2	Point-3	Point-4	Point-5	Point-6
O	3.175	6.570	19.001	0.582	4.277	3.136
W	15.659	12.812	5.701	15.298	14.472	7.899
C	1.641	20.871	3.208	1.099	7.319	3.318
Ti	18.576	3.454	67.105	0.831	17.951	0.348
Cr	13.154	3.468	0.730	3.545	3.237	70.436
B	0.000	0.000	0.000	0.000	0.000	0.000
Si	1.133	8.224	0.332	0.384	1.159	0.857
Ni	46.662	44.601	3.922	78.861	51.585	14.005
Total	100.000	100.000	100.000	100.000	100.000	100.000

Fig. 12. SEM photograph and EDS analysis of the worn surface of S20 composite sample.

rated from the composite surface and their free movement on the contact interface.

CONFLICT OF INTEREST

The authors declare that they have no conflict of interest.

REFERENCES

1. Neville, A., Reza, F., Chiovelli, S., and Revega, T., Assessing metal matrix composites for corrosion and erosion-corrosion applications in the oil sands industry, *Corrosion,* 2006, vol. 62, no. 8, pp. 657–675. https://doi.org/10.5006/1.3278293
2. Tjong, S.C. and Ma, Z.Y., Microstructural and mechanical characteristics of in situ metal matrix composites, *Mater. Sci. Eng., R,* 2000, vol. 29, nos. 3–4, pp. 49–113. https://doi.org/10.1016/S0927-796X(00)00024-3
3. Wang, J. and Fu, S., Production of in situ vanadium carbide particulate reinforced iron matrix composite, *Mater. Sci.,* 2014, vol. 20, no. 4, pp. 409–413. https://doi.org/10.5755/j01.ms.20.4.6445
4. Serres, N., Hlawka, F., Costil, S., Langlade, C., and Machi, F., Microstructures and mechanical properties of metallic NiCrBSi and composite NiCrBSi-WC layers manufactured via hybrid plasma/laser process, *Appl. Surf. Sci.,* 2011, vol. 257, no. 12, pp. 5132–5137. https://doi.org/10.1016/j.apsusc.2010.11.062
5. Bin, C.A.I., Tan, Y.F., Long, H.E., Hua, T.A.N., and Li, G.A.O., Tribological properties of TiC particles reinforced Ni-based alloy composite coatings, *Trans. Nonferrous Met. Soc. China,* 2013, vol. 23, no. 6, pp. 1681–1688. https://doi.org/10.1016/S1003-6326(13)62648-5
6. Buytoz, S., Ulutan, M., Islak, S., Kurt, B., and Çelik, O.N., Microstructural and wear characteristics of high velocity oxygen fuel (HVOF) sprayed NiCrBSi-

SiC composite coating on SAE 1030 steel, *Arabian J. Sci. Eng.,* 2013, vol. 38, no. 6, pp. 1481–1491. https://doi.org/10.1007/s13369-013-0536-y

7. Zikin, A., Antonov, M., Hussainova, I., Katona, L., and Gavrilović, A., High temperature wear of cermet particle reinforced NiCrBSi hardfacings, *Tribol. Int.,* 2013, vol. 68, pp. 45–55. https://doi.org/10.1016/j.triboint.2012.08.013
8. Ma, J., Yang, J., Bi, Q., and Liu, W., Dry-sliding tribological behavior of Fe–28Al–5Cr/TiC composites, *Wear,* 2011, vol. 271, nos. 5–6, pp. 881–888. https://doi.org/10.1016/j.wear.2011.03.020
9. Zhang, X., Ma, J., Fu, L., Zhu, S., Li, F., Yang, J., and Liu, W., High temperature wear resistance of Fe–28Al–5Cr alloy and its composites reinforced by TiC, *Tribol. Int.,* 2013, vol. 61, pp. 48–55. https://doi.org/10.1016/j.triboint.2012.12.005
10. Gómez-del Rio, T., Garrido, M.A., Fernández, J.E., Cadenas, M., and Rodriguez, J., Influence of the deposition techniques on the mechanical properties and microstructure of NiCrBSi coatings, *J. Mater. Process. Technol.,* 2008, vol. 204, nos. 1–3, pp. 304–312. https://doi.org/10.1016/j.jmatprotec.2007.11.042
11. Miguel, J.M., Guilemany, J.M., and Vizcaino, S., Tribological study of NiCrBSi coating obtained by different processes, *Tribol. Int.,* 2003, vol. 36, no. 3, pp. 181–187. https://doi.org/10.1016/S0301-679X(02)00144-5
12. Niranatlumpong, P. and Koiprasert, H., Phase transformation of NiCrBSi-WC and NiBSi-WC arc sprayed coatings, *Surf. Coat. Technol.,* 2011, vol. 206, nos. 2–3, pp. 440–445. https://doi.org/10.1016/j.surfcoat.2011.07.057
13. Tobar, M.J., Alvarez, C., Amado, J.M., Rodríguez, G., and Yanez, A., Morphology and characterization of laser clad composite NiCrBSi-WC coatings on stainless steel, *Surf. Coat. Technol.,* 2006, vol. 200, nos. 22–23, pp. 6313–6317. https://doi.org/10.1016/j.surfcoat.2005.11.093
14. Gonzalez, R., Cadenas, M., Fernández, R., Cortizo, J.L., and Rodríguez, E., Wear behavior of flame sprayed NiCrBSi coating remelted by flame or by laser, *Wear,* 2007, vol. 262, nos. 3–4, pp. 301–307. https://doi.org/10.1016/j.wear.2006.05.009
15. Jia, J., Lu, J., Zhou, H., and Chen, J., Tribological behavior of Ni-based composite under distilled water lubrication, *Mater. Sci. Eng., A,* 2004, vol. 381, nos. 1–2, pp. 80–85. https://doi.org/10.1016/j.msea.2004.03.059
16. Properties and Selection: Nonferrous Alloys and Special-Purpose Materials, vol. 2 of *ASM Handbook*, Davis, J.R., Ed., Materials Park, OH: ASM Int., 1990.
17. Onuoha, C.C., Kipouros, G.J., Farhat, Z.N., and Plucknett, K.P., The reciprocating wear behavior of TiC–304L stainless steel composites prepared by melt infiltration, *Wear,* 2013, vol. 303, nos. 1–2, pp. 321–333. https://doi.org/10.1016/j.wear.2013.03.040
18. Akhtar, F., Microstructure evolution and wear properties of in situ synthesized TiB_2 and TiC reinforced steel matrix composites, *J. Alloys Compd.,* 2008, vol. 459, nos. 1–2, pp. 491–497. https://doi.org/10.1016/j.jallcom.2007.05.018
19. Karantzalis, A.E., Lekatou, A., and Tsirka, K., Solidification observations and sliding wear behavior of vacuum arc melting processed Ni–Al–TiC composites, *Mater. Charact.,* 2012, vol. 69, pp. 97–107. https://doi.org/10.1016/j.matchar.2012.04.013
20. Russias, J., Cardinal, S., Aguni, Y., Fantozzi, G., Bienvenu, K., and Fontaine, J., Influence of titanium nitride addition on the microstructure and mechanical properties of TiC-based cermets, *Int. J. Refract. Met. Hard Mater.,* 2005, vol. 23, nos. 4–6, pp. 358–362. https://doi.org/10.1016/j.ijrmhm.2005.05.008
21. Wang, H., Zhang, R., Hu, X., Wang, C.A., and Huang, Y., Characterization of a powder metallurgy SiC/Cu–Al composite, *J. Mater. Process. Technol.,* 2008, vol. 197, nos. 1–3, pp. 43–48. https://doi.org/10.1016/j.jmatprotec.2007.06.002
22. Wang, Y., Zhang, X., Zeng, G., and Li, F., In situ production of Fe–VC and Fe–TiC surface composites by cast-sintering, *Composites, Part A,* 2001, vol. 32, no. 2, pp. 281–286. https://doi.org/10.1016/S1359-835X(00)00118-4
23. Rahimian, M., Ehsani, N., Parvin, N., and Baharvandi, H.R., The effect of sintering temperature and the amount of reinforcement on the properties of Al–Al_2O_3 composite, *Mater. Des.,* 2009, vol. 30, no. 8, pp. 3333–3337. https://doi.org/10.1016/j.matdes.2008.11.027
24. Kang, H.K., Microstructure and electrical conductivity of high volume Al_2O_3-reinforced copper matrix composites produced by plasma spray, *Surf. Coat. Technol.,* 2005, vol. 190, p. 448–552. https://doi.org/10.1016/j.surfcoat.2004.02.002
25. Islak, S., Çelik, E., Kir, D., and Özorak, C., Characterization of hot pressed CuAl–TiC composites with different TiC grain sizes, *Russ. J. Non-Ferrous Met.,* 2016, vol. 57, no. 4, pp. 374–380. https://doi.org/10.3103/S1067821216040040
26. da Silva, L.J., Scheuer, C.J., and D'Oliveira, A.S.C., Effect of microstructure on wear performance of NiCrSiBC coatings, *Wear,* 2019, vols. 428–429, pp. 387–394. https://doi.org/10.1016/j.wear.2019.04.005
27. Islak, S., Kir, D., and Buytoz, S., Effect of sintering temperature on electrical and microstructure properties of hot-pressed Cu–TiC composites, *Sci. Sintering,* 2014, vol. 46, no. 1, pp. 15–21. https://doi.org/10.2298/SOS1401015I
28. Efe, G.C., Ipek, M., Zeytin, S., and Bindal, C., An investigation of the effect of SiC particle size on Cu–SiC composites, *Composites, Part B,* 2012, vol. 43, no. 4, pp. 1813–1822. https://doi.org/10.1016/j.compositesb.2012.01.006
29. Ngai, T.L., Zheng, W., and Li, Y., Effect of sintering temperature on the preparation of Cu–Ti_3SiC_2 metal matrix composite, *Prog. Nat. Sci.: Mater. Int.,* 2013, vol. 23, no. 1, pp. 70–76. https://doi.org/10.1016/j.pnsc.2013.01.011

30. Shu, K.M. and Tu, G.C., The microstructure and the thermal expansion characteristics of Cu/SiCp composites, *Mater. Sci. Eng., A,* 2003, vol. 349, nos. 1–2, pp. 236–247. https://doi.org/10.1016/S0921-5093(02)00788-8
31. Kumar, G.V., Rao, C.S.P., and Selvaraj, N., Mechanical and tribological behavior of particulate reinforced aluminum metal matrix composites—a review, *J. Miner. Mater. Charact. Eng.,* 2011, vol. 10, no. 1, pp. 59–91. https://doi.org/10.4236/jmmce.2011.101005
32. Bin, C.A.I., Tan, Y.F., Hua, T.A.N., Jing, Q.F., and Zhang, Z.W., Tribological behavior and mechanism of NiCrBSi–Y_2O_3 composite coatings, *Trans. Nonferrous Met. Soc. China,* 2013, vol. 23, no. 7, pp. 2002–2010. https://doi.org/10.1016/S1003-6326(13)62689-8
33. Stoica, V., Ahmed, R., Itsukaichi, T., and Tobe, S., Sliding wear evaluation of hot isostatically pressed (HIPed) thermal spray cermet coatings, *Wear,* 2004, vol. 257, no. 11, pp. 1103–1124. https://doi.org/10.1016/j.wear.2004.07.016
34. Bailey, R. and Sun, Y., Unlubricated sliding friction and wear characteristics of thermally oxidized commercially pure titanium, *Wear,* 2013, vol. 308, nos. 1–2, pp. 61–70. https://doi.org/10.1016/j.wear.2013.09.020
35. Krishna, D.S.R., Brama, Y.L., and Sun, Y., Thick rutile layer on titanium for tribological applications, *Tribol. Int.,* 2007, vol. 40, no. 2, pp. 329–334. https://doi.org/10.1016/j.triboint.2005.08.004
36. Yetim, A.F., Investigation of wear behavior of titanium oxide films, produced by anodic oxidation, on commercially pure titanium in vacuum conditions, *Surf. Coat. Technol.,* 2010, vol. 205, no. 6, pp. 1757–1763. https://doi.org/10.1016/j.surfcoat.2010.08.079